Jurnal Teknologi

Full Paper

THE ENHANCED PHOTOCATALYTIC PROPERTIES OF SILVER PHOSPHATE SYNTHESIZED UNDER MANGOSTEEN PEEL EXTRACT SOLUTION

Alfa Marcorius[a], Uyi Sulaeman[a*], Mohammad Afif[a], Siti Nurfiah[a], Khanifudin Khanifudin[b], Khusnul Afifah[a]

[a]Department of Chemistry, Faculty of Mathematics and Natural Sciences, Jenderal Soedirman University, Purwokerto 53123, Indonesia
[b]Department of Mathematics, Faculty of Mathematics and Natural Sciences, Jenderal Soedirman University, Purwokerto, 53123, Indonesia

Article history
Received
29 March 2021
Received in revised form
27 September 2021
Accepted
7 October 2021
Published Online
20 December 2021

*Corresponding author
sulaeman@unsoed.ac.id

Graphical abstract

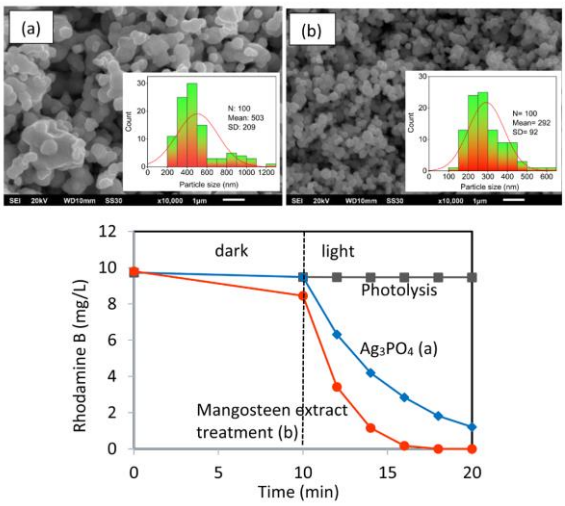

Abstract

The synthesis of silver phosphate (Ag_3PO_4) photocatalyst has been widely developed for organic pollutant degradation. However, the large particle of this photocatalyst limits the photocatalytic activity. The smaller particle size of the Ag_3PO_4 photocatalyst was successfully prepared using the starting material of $AgNO_3$ and $Na_2HPO_4.12H_2O$ under mangosteen peel extract solution. The starting materials were dissolved in mangosteen peel extract solutions prepared at the concentration of 1% (w/v). The reaction of silver nitrate and phosphate solution was conducted at room temperature. The samples of pristine Ag_3PO_4 and Ag_3PO_4 prepared under mangosteen peel extract were studied using XRD, DRS, SEM, BET, and FTIR. All photocatalytic activities were evaluated using Rhodamine B photooxidation under blue light irradiation (LED, 3 Watt). The results showed that the mangosteen peel extract significantly decreased the particle size, lowered the bandgap energy from 2.12 to 2.00 eV, and increased the crystallinity of Ag_3PO_4. The interaction of xanthones from mangosteen peel extract solution with silver ion might affect the growth particle of Ag_3PO_4, and inhibit the agglomeration leading to small particle size, more uniform distribution, high crystallinity, and low bandgap energy. These properties enhanced the photocatalytic activity up to 2.9 times higher compared to the sample without the treatment of mangosteen peel extract.

Keywords: Silver phosphate, mangosteen peel, photocatalysis, Rhodamine B, particle size

1.0 INTRODUCTION

Today silver orthophosphate has been developed as a photocatalyst for dye removal under visible light exposure due to owing small bandgap energy of 2.43 eV, strong photooxidation, and high quantum yield [1, 2]. This material can be an alternative photocatalyst that is active in visible light in addition to popular photocatalysts such as N-TiO_2 [3-5]. The modifications of morphology in Ag_3PO_4 photocatalyst have been applied to improve their photocatalytic activity [6]. Morphology of coral-like microspheres [7],

branched Ag_3PO_4 crystals with porous structure [8] and truncated tetragonal bipyramids [9] had improved the photocatalytic activity of Ag_3PO_4. The changed morphology can influence the activity due to a different facet of Ag_3PO_4. However, design a particular morphology that has high activity is very difficult in Ag_3PO_4.

The impressive improvement of photocatalytic activity can be achieved through dopant incorporation on the surface of Ag_3PO_4. The dopant of sulfate [10], platinum complex [11], bismuth [12], molybdenum [13], nickel [14], and lanthanum [15] could be applied in Ag_3PO_4. The metallic silver dopant on Ag_3PO_4 is the most promising because it can be created through a simple reduction of Ag^+ ions [16]. This dopant could also generate the surface plasmon resonance that leads to a highly active photocatalyst [17]. However, most of these designs have used large particles of Ag_3PO_4.

Modification of Ag_3PO_4 into composite photocatalysts has also significantly improved photocatalytic activity. Generating electron excitation could effectively be facilitated in a hybrid photocatalyst [18], p-n heterojunction [19], and Z-scheme mechanism [20] which can boost the photocatalytic ability. The formation of g-C_3N_4/Ag_3PO_4 hybrid can maintain the Ag_3PO_4 from dissolution in water [21]. It leads to higher stability of activity. The composite of Ag_3PO_4/$CdWO_4$ photocatalyst improved the separation of carrier pairs through a p-n junction that increase the efficiency of activity [22]. The p–n junction and piezoelectric effect can also be designed through Ag_3PO_4/ZnO composite [23]. Under this modification, the piezoelectric effect of ZnO can be generated which leads to the improvement of pollutant degradation. The composite can also generate a Z-scheme mechanism, Ag_3PO_4 and C_3N_5 can be a good model of this system [24]. Through this mechanism, the photocatalytic ability can be improved significantly. However, up to now, the large particle of Ag_3PO_4 has been still a problem in the Ag_3PO_4-based composites that lead to limitation of photocatalytic activity.

The photocatalytic activity of Ag_3PO_4 is strongly affected by the size and surface area [25]. The large particle size could have a low surface area that leads to the poor performance of Ag_3PO_4 activity. Therefore, the development of Ag_3PO_4 synthesis to produce a small particle size is very important. Many researchers have developed the high surface area of Ag_3PO_4. Attaching the graphene oxide aerogel on Ag_3PO_4 increased the specific surface area and adsorption ability leading to high photocatalytic activity [26]. The higher content of graphene oxide aerogel showed a higher adsorption capacity. The mesoporous TiO_2 spheres could also be applied to enhance the surface area of Ag_3PO_4 [27]. The large pores and high specific surface area could lead to high photocatalytic activity due to higher adsorption capacity.

Recently, the green synthesis and plant-mediated materials synthesis is very interesting due to the eco-friendly approach that brings to high efficiency [28,29]. Mangosteen peel, a natural dye, might be applied for an agent of synthesis due to containing xanthone [30] that has polyphenol groups. This compound has derivatives of α-mangostin, β-mangostin, γ-mangostin, 3-isomangostin hydrate, 8-deoxygartanin, gartanin, garcinone E, and hydroxycalabaxanthone [31].

Herein, the mangosteen peel extract solution was applied to affect the coprecipitation of Ag_3PO_4 synthesis. A polyphenol of xanthone might control the crystal growth and morphology during the precipitation. This treatment improved the crystallinity, increased the surface area, and lowered the bandgap energy of Ag_3PO_4.

2.0 METHODOLOGY

2.1 Materials

The chemical of disodium hydrogen phosphate dodecahydrate ($Na_2HPO_4.12H_2O$), silver nitrate ($AgNO_3$), Rhodamine B, ammonium oxalate, benzoquinone, and isopropanol are pro analysis and purchased from Merck. The mangosteen peel extracts are provided using the extraction of the mangosteen peel using methanol [32].

2.2 Synthesis of Photocatalysts

The silver phosphates were synthesized using simple coprecipitation of $AgNO_3$ and $Na_2HPO_4.12H_2O$ [18] under mangosteen peel extract solution. To preparing the mangosteen peel extracts, fresh mangosteen peel was washed with water and dried in the open air for 3 days. Dried mangosteen peel (10 gram) was ground and immersed in 1 liter of methanol for 24 h. The filtrate was separated and evaporated under a rotatory evaporator at 64.7°C. The mangosteen peel extract solution was prepared by adding 1 gram of extract with water of 100 mL solution (1% of w/v). The sample without and with mangosteen extract solution was named M-0 and M-100, respectively.

The photocatalysts were prepared by mixing two solutions of $AgNO_3$ and sodium phosphate containing mangosteen peel extract. The $AgNO_3$ solution was made by dissolving 1.7 g of $AgNO_3$ in 10 mL of mangosteen peel extract solution, whereas the sodium phosphate solution was prepared by dissolving 1.2 g of $Na_2HPO_4.12H_2O$ in 20 ml of mangosteen peel extract solution. The two solutions were then mixed under stirring at 500 rpm for 10 minutes. The products were filtered and washed with water and dried at 60°C for 3 h.

2.3 Characterization

The sample of pristine Ag_3PO_4 (M-0) and Ag_3PO_4 prepared under mangosteen peel extract (M-100) were studied using XRD (Shimadzu XRD-7000) to investigate the structure of photocatalysts. The peak of XRD was further analyzed by HighScore Plus. The absorption and bandgap energies of photocatalyst were investigated using diffuse reflectance spectroscopy, DRS (Shimadzu UV–2450). The direct transition was applied to estimate the bandgap energy of samples. Morphologies of samples were observed using SEM (JEOL JSM-6510LA). The surface area and pore size were evaluated using the BET analysis (Quantachrome Instruments version 11.0). FTIR (Shimadzu Prestige-21) was used to investigate the functional group of samples.

2.4 Photocatalytic Activity Evaluation

The photocatalytic activity was studied using Rhodamine B (RhB) photodecomposition [16]. Typically, 0.1 g of catalyst was dispersed in 100 mL of 10 mg/L Rhodamine B solution. This solution was irradiated under blue light (LED 3W, Ranpo) irradiation after 10 minutes in dark conditions. The concentration of Rhodamine B was monitored by a UV-Vis spectrophotometer at 554 nm (33).

The photocatalytic reactions were evaluated using the pseudo-first-order kinetic with the rate constant (k) using the equation of $\ln(C_0/C) = kt$, where C_0 is the initial concentration and C is the concentration at t time [34]. Linear relationships between $\ln(C_0/C)$ and reaction time (t) implying that the reactions are fit with the pseudo-first-order kinetics.

The mechanism of photocatalytic was investigated using ammonium oxalate, benzoquinone, and isopropanol as a scavenger for holes, superoxide ion radicals, and hydroxyl radicals, respectively [16]. In this experiment, 1 mmol/L of scavenger was applied in Rhodamine B solution. Their effects on photocatalytic activity of RhB degradation in M-0 and M-100, were investigated after 15 minutes of illumination. The RhB degradation (%) was calculated by the equation of $((C_0-C_{15})/C_0)x100\%$, where C_0 and C_{15} are the initial concentration and 15 minutes photodegradation, respectively.

3.0 RESULTS AND DISCUSSION

3.1 Characterization of Photocatalysts

The photocatalyst of pristine Ag_3PO_4 (M-0) and the Ag_3PO_4 prepared using the mangosteen peel extract (M-100) were characterized using the XRD, SEM, BET, and DRS. Figure 1 shows the XRD profile of M-0 and M-100. These samples were identified as body-centered cubic structures (JCPDS No. 06-0505) [35]. No impurities were observed in both M-0 and M-100, indicating that the catalysts are single phases. However, higher intensities of XRD peaks could be observed in M-100, reflecting that the mangosteen peel extract solution could enhance the crystallinity of the sample. It is similar to the function of surfactants on ZnO nanoparticles that increases the crystallinity of the photocatalyst [36]. The calculated measurement of XRD can be summarized in Table 1. The decreased peak position and lowered full width at half maximum (FWHM) were found in the sample of M-100. The increase of d-space in M-100 indicating the expansion of the crystal occurred. Based on these differences, mangosteen peel extracts significantly affected the crystallite size, lattice strain, and crystallinity of Ag_3PO_4.

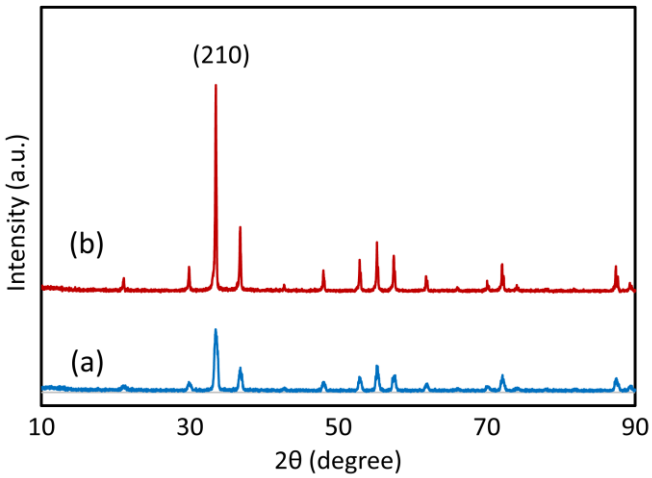

Figure 1 The XRD of pristine Ag_3PO_4 (M-0) (a) and Ag_3PO_4 synthesized under mangosteen peel extract (M-100) (b)

Table 1 The characteristics of peak (210) in XRD analysis

Samples	Peak position (deg)	Height (counts)	FWHM (deg)	d-space (Å)
M-0	33.51842	364.6622	0.44698	2.6714
M-100	33.47597	1169.762	0.16127	2.6747

Figure 2(a) demonstrated that the pristine Ag_3PO_4 (M-0) possesses an irregular shape of 200–600 nm in diameter with an average of 503 nm. The addition of mangosteen peel extract on the preparation decreases the particle size significantly up to 150–350 nm with an average size of 292 nm (Figure 2(b)). It indicates that the mangosteen peel extract could control the grain growth of particles. The interaction of xanthone and its derivatives from extract solution and silver ion might affect the growth particle of Ag_3PO_4, and inhibit the agglomeration leading to a small particle size formation and more uniform distribution.

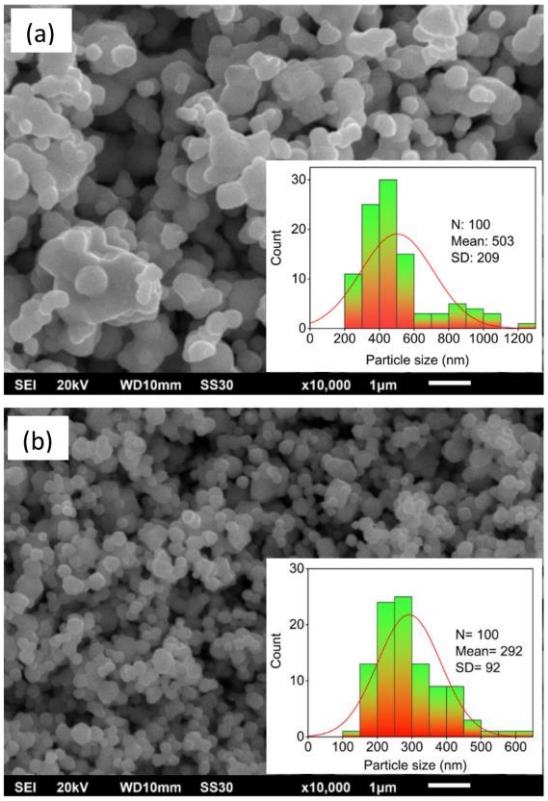

Figure 2 SEM images and the insert of particle size distribution histogram of pristine Ag_3PO_4 (M-0) (a) and Ag_3PO_4 prepared by mangosteen peel extract (M-100) (b)

N_2 adsorption-desorption isotherm was conducted to investigate the pore structure of M-0 and M-100. M-0 possesses a specific surface area of 1.42 m^2/g and a total pore volume of 0.0033 cm^3/g, while the specific surface area of M-100 was 3.39 m^2/g with a total pore volume of 0.0063 cm^3/g. As expected, the M-100 exhibited higher surface area and pore volume compared to M-0. The pore size distribution of M-0 and M-100 was estimated via the Barrett–Joyner–Halenda (BJH) method (Figure 3).

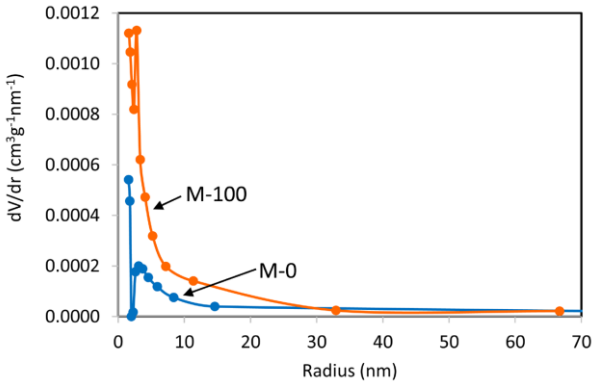

Figure 3 BET pore size distribution curves for pristine Ag_3PO_4 (M-0) and with mangosteen peel extract (M-100)

The pore size distribution of M-0 revealed mostly centered at 2–15 nm with an average pore size of 4.6 nm, whereas the pore size distribution of M-100 was mostly centered at 2–25 nm with an average pore size of 3.7 nm. The corresponding pore size distribution indicates that the photocatalysts were mesopores. The characterization of BET analysis can be seen in Table 2.

Table 2 The surface area, average pore radius, and total pore of samples

Samples	S_{BET} (m^2/g)	Average pore Radius (nm)	Total Pore Volume (cm^3/g)
M-0	1.42	4.6	0.0033
M-100	3.39	3.7	0.0063

Figure 4 showed that the absorption of M-100 was higher compared to the M-0, indicating the mangosteen peel extract affected the optical properties of Ag_3PO_4. The bandgap energy can be calculated using the formula (1):

$$(Ahv)^2 = hv - E_g \qquad (1)$$

where *Eg, v, h,* and *A* were bandgap energy, light frequency, Planck constant, and absorbance, respectively [37]. The bandgap energies of 2.12 eV and 2.00 eV were estimated for the M-0 and M-100, respectively. The lower bandgap energy of M-100 might be the effect of the chemical interaction of functional group from xanthone structure of mangosteen peel extract with the precursors during the coprecipitation of Ag_3PO_4 that increases the crystallinity. It is reported that the increased crystallinity can lower the bandgap energy [38]. The effect of mangosteen on the bandgap energy is also found in TiO_2 [39].

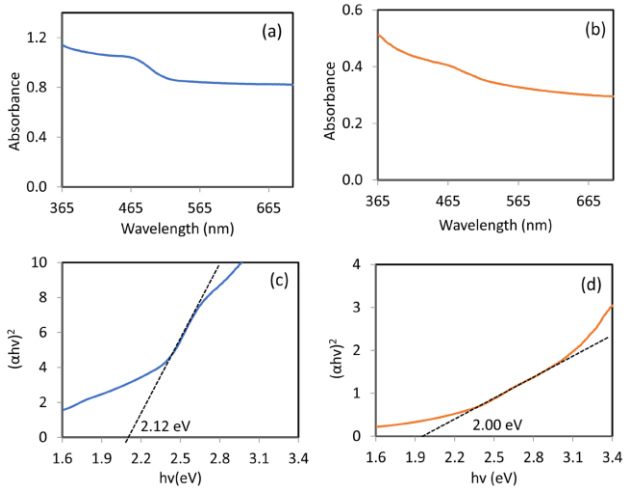

Figure 4 The absorption of M-0 (a) and M-100 (b) and their bandgap calculation of M-0 (c) and M-100 (d)

The FTIR spectra of pristine Ag_3PO_4 (M-0) and Ag_3PO_4 prepared under mangosteen peel extract (M-100) were scanned from 400 cm^{-1} to 4000 cm^{-1}, the results are shown in Figure 5. For pristine Ag_3PO_4 (M-0), the peaks at 563 cm^{-1}, 1010 cm^{-1}, and 1385 cm^{-1} are assigned to O=P-O bending vibration, P-O-P asymmetric stretching, and nitrate impurities, respectively [40]. The broad peak at around 3431 cm^{-1} is attributed to O-H stretching vibration, whereas the peak at 1656 cm^{-1} is attributed to H-O-H bending vibration from water adsorbed on the surface of Ag_3PO_4 [41]. The spectrum of M-100 is slightly different from the spectrum of M-0. A slight shift of spectrum in M-100 was found at 3433 cm^{-1}, 1658 cm^{-1}, and 1012 cm^{-1} that come from the stretching vibration of O-H groups, H-O-H bending vibrations, and asymmetric stretching of P-O-P, respectively. The O-H stretching vibration of M-100 was of higher intensity compared to the M-0, indicating that the extract of mangosteen peel affected the vibration spectrum of the photocatalyst.

However, the vibrations of C-O ester (1027 cm^{-1}), C=O stretching (1686 cm^{-1}), -CH_3 bending (1363 cm^{-1}), CH_2- bending (1419 cm^{-1}), and C-H sp^3 stretching (2938 and 2828 cm^{-1}) [42] from derivative xanthone were not observed due to releasing the mangosteen peel extract form Ag_3PO_4 surface due to washing treatment during the synthesis. It indicates the extract might act as a precipitating agent of particle size and crystallinity control, similar to the role of $H_2C_2O_4$ and Na_2CO_3 for the preparation of bismuth oxide [43].

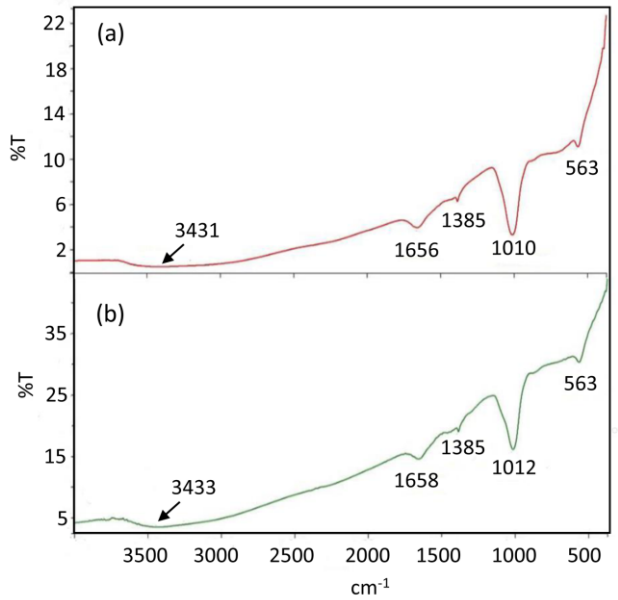

Figure 5 The FTIR of pristine Ag_3PO_4 (M-0) (a) and Ag_3PO_4 prepared under mangosteen peel extract solution (M-100) (b)

3.2 Photocatalytic Evaluation

The photocatalytic activities of M-0 and M-100 were investigated under blue light irradiation (Figure 6). The samples of Ag_3PO_4 synthesized under mangosteen peel extract solution showed higher photocatalytic activity. A decrease of photocatalytic activity during the dark reaction of extract-treated samples indicating there is an adsorption phenomenon on the surface of the photocatalyst.

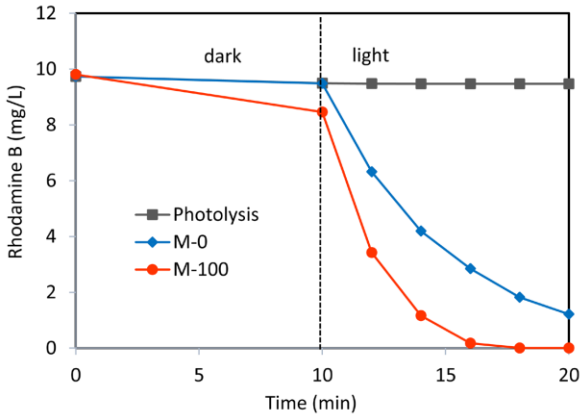

Figure 6 The photocatalytic activity of pristine Ag_3PO_4 (M-0) and Ag_3PO_4 synthesized under mangosteen peel extract (M-100)

The photocatalytic activity evaluation shows that the rate constant of 0.202, and 0.587 min^{-1} had been calculated in the sample of M-0 and M-100, respectively. The rate constant increased 2.9 times higher compared to the sample of M-0. The excellent photocatalytic activity of M-100 might be induced by higher surface area, pore volume, and crystallinities.

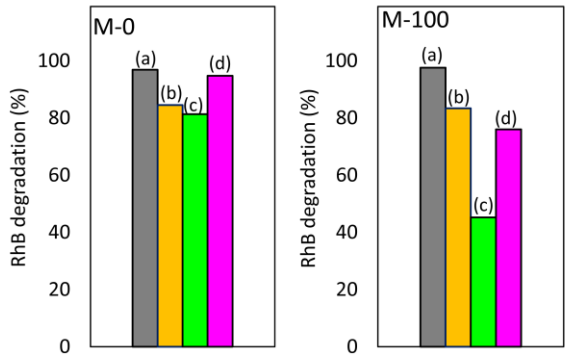

Figure 7 Mechanism analysis of the photocatalytic activity of Ag_3PO_4 (M-0) and Ag_3PO_4 synthesized under mangosteen peel extract solution (M-100), using (a) control, (b) ammonium oxalate, (c) benzoquinone, and (d) isopropanol scavenger for investigating the holes, superoxide ion (O_2^{-}•), and hydroxyl (•OH), respectively

The mechanism of photocatalysis was investigated by adding ammonium oxalate, benzoquinone, and isopropanol in a photocatalytic reaction as a scavenger to investigate the existence of holes (h^+), superoxide ion (O_2^{-}•) radical, and

hydroxyl (•OH) radical, respectively [16]. The sample of M-0 and M-100 were evaluated in detail, the results can be seen in Figure 7. The ammonium oxalate and benzoquinone addition on the M-0 photocatalyst suppressed the photocatalytic activity, indicating that the holes and superoxide ion radical are significant roles in the M-0, whereas the isopropanol addition did not suppress the reaction reflecting that the reaction was not run via hydroxyl radical. In contrast, the addition of ammonium oxalate, benzoquinone, and isopropanol on M-100 suppressed the reaction significantly, suggesting that the reaction was run via hole, superoxide radical, and hydroxyl radical. It showed that the superoxide radical was the most prominent in the mechanism of the M-100 photocatalyst. The high superoxide radical in M-100 might be generated due to lower bandgap energy. This property increases the photoexcited electron in the conduction band leading to higher oxygen reduction in the surface of Ag_3PO_4.

4.0 CONCLUSION

The Ag_3PO_4 was successfully synthesized using coprecipitation of $AgNO_3$ and $Na_2HPO_4.12H_2O$ under mangosteen peel extract solution. The extract has significantly affected the coprecipitation of Ag_3PO_4 that leads to a higher crystallinity, smaller particle size, and higher surface area. The interaction of xanthone and its derivatives from mangosteen peel extract might affect the growth particle of Ag_3PO_4 and inhibit the agglomeration leading to small particle size, more uniform distribution, high crystallinity, and low bandgap energy. The photocatalytic ability of Ag_3PO_4 can be improved, the rate is 2.9 times higher compared to the pristine Ag_3PO_4. The enhanced photocatalytic activity might be generated by the higher formation of superoxide ions and hydroxyl radicals in photocatalytic reactions.

Acknowledgment

This research was financially supported by the Student Creativity Program for Research Activity and the World Class Research Program of the Republic of Indonesia (117/SP2H/LT/DRPM/2021).

References

[1] Yi, Z., J. Ye, N. Kikugawa, T. Kako, S. Ouyang, H. Stuart-Williams, H. Yang, J. Cao, W. Luo, and Z. Li. 2010. An Orthophosphate Semiconductor with Photooxidation Properties Under Visible-light Irradiation. *Nature Materials.* 9: 559-564. https://doi.org/10.1038/nmat2780.

[2] Chen, X., X. Huang, and Z. Yi. 2014. Enhanced Ethylene Photodegradation Performance of g-C_3N_4–Ag_3PO_4 Composites with Direct Z-scheme Configuration. *Chemistry-A European Journal.* 20: 17590-17596. https: //doi.org/10.1002/chem.201404284.

[3] Hidayanto, E., H. Sutanto, Mukholit, S. Wibowo, and M. Irwanto. 2017. Morphology and Degradation Kinetics of N-Doped TiO_2 Nano Particle Synthesized using Sonochemical Method. *Solid State Phenomena*. 266: 95-100. https: //doi.org/10.4028/www.scientific.net/SSP.266.95.

[4] Sutanto, H., E. Hidayanto, Mukholit, S. Wibowo, I. Nurhasanah, and Hadiyanto. 2017. The Physical and Photocatalytic Properties of N-doped TiO_2 Polycrystalline Synthesized by a Single Step Sonochemical Method at Room Temperature. *Materials Science Forum*. 890: 121-126. https://doi.org/10.4028/www.scientific.net/MSF.890.121.

[5] Pandiangan, I. F. D., H. Sutanto, and I. Nurhasanah. 2018. Effect of Annealing Temperature on Optical Properties and Photocatalytic Properties of TiO_2:N 8% Thin Film for Rhodamine B Degradation. *Materials Research Express*. 5(8): 086404. https://doi.org/10.1088/2053-1591/aad15d.

[6] Afifah, K., R. Andreas, D. Hermawan, and U. Sulaeman. 2019. Tuning the Morphology of Ag_3PO_4 Photocatalysts with an Elevated Concentration of KH_2PO_4. *Bulletin of Chemical Reaction Engineering & Catalysis*. 14(3): 625-633. https://doi.org/10.9767/bcrec.14.3.4649.625-633.

[7] Zheng, C., H. Yang, and Y. Yang. 2017. Synthesis of Novel Coral-like Ag_3PO_4 Microspheres under the Aid of Trisodium Citrate and Acetic Acid. *Journal of the Ceramic Society of Japan*. 125: 141-144. https://doi.org/10.2109/jcersj2.16313.

[8] Dong, P., Y. Wang, H. Li, H. Li, X. Ma, and L. Han. 2013. Shape-controllable Synthesis and Morphology-dependent Photocatalytic Properties of Ag_3PO_4 Crystals. *Journal of Materials Chemistry* A. 1: 4651-4656. https://doi.org /10.1039/C3TA00130J.

[9] Xu, Y. and W. Zhang. 2013. Morphology-controlled Synthesis of Ag_3PO_4 Microcrystals for High Performance Photocatalysis. *CrystEngComm*. 15: 5407-5411. https: //doi.org/10.1039/C3CE40172C.

[10] Panthi, G., M. M. Hassan, Y. S. Kuk , J. Y. Kim, H. J. Chung, S. T. Hong, and M. Park. 2020. Enhanced Antibacterial Property of Sulfate-doped Ag_3PO_4 Nanoparticles Supported on PAN Electrospun Nanofibers. *Molecules*. 25(6): 1411. https://doi.org/10.3390/molecules25061411.

[11] U. Sulaeman, R. D. Permadi, D. R. Ningsih, H. Diastuti, A. Riapanitra, and S. Yin. 2020. The Surface Modification of Ag_3PO_4 using Anionic Platinum Complexes for Enhanced Visible-light Photocatalytic Activity. *Materials Letters*. 259: 126848. https://doi.org/10.1016/j.matlet.2019.126848.

[12] Zhang, S., S. Zhang, and L. Song. 2014. Super-high Activity of Bi^{3+} Doped Ag_3PO_4 and Enhanced Photocatalytic Mechanism. *Applied Catalysis B: Environmental*. 152-153: 129-139. https://doi.org/10.1016/j.apcatb.2014.01.020.

[13] Hussien, M. S. A. and I. S. Yahia. 2018. Visible Photocatalytic Performance of Nanostructured Molyb Denum-doped Ag_3PO_4: Doping Approach. *Journal of Photochemistry and Photobiology A: Chemistry*. 356: 587-594. https://doi.org/10.1016/j.jphotochem.2018.01.026.

[14] Song, L., Z. Chen, T. Li, and S. Zhang. 2017. A Novel Ni^{2+}-Doped Ag_3PO_4 Photocatalyst with High Photocatalytic Activity and Enhancement Mechanism. *Materials Chemistry and Physics*. 186: 271-279. https://doi.org /10.1016/j.matchemphys.2016.10.053.

[15] Xie Y. P. and G. S. Wang. 2014. Visible Light Responsive Porous Lanthanum-doped Ag_3PO_4 Photocatalyst with High Photocatalytic Water Oxidation Activity. *Journal of Colloid and Interface Science*. 430: 1-5. https://doi.org /10.1016/j.jcis.2014.05.020.

[16] Sulaeman, U., S. Suhendar, H. Diastuti, R. Andreas, and S. Yin. 2020. Design of Defect and Metallic Silver in Silver Phosphate Photocatalyst using the Hydroxyapatite and Glucose. *Indonesian Journal of Chemistry*. 20 (6): 1441-1447. https://doi.org/10.22146/ijc.48647.

[17] Gondal, M. A., X. Chang, W. E. I. Sha, Z. H. Yamani and Q. Zhou. 2013. Enhanced Photoactivity on Ag/Ag_3PO_4 Composites by Plasmonic Effect. *Journal of Colloid and*

Interface Science. 392: 325-330. https://doi.org/10.1016/j.jcis.2012.09.086

[18] Sulaeman, U., B. Liu, S. Yin, and T. Sato. 2017. Synthesis of Ag_3PO_4 using Hydrophilic Polymer and Their Photocatalytic Activities Under Visible Light Irradiation. *Bulletin of Chemical Reaction Engineering & Catalysis*. 12(2): 206-211. http://dx.doi.org/10.9767/bcrec.12.2.767.206-211.

[19] Teng, W., X. Tan, X. Li, and Y. Tang. 2017. Novel Ag_3PO_4/MoO_3 p-n Heterojunction with Enhanced Photocatalytic Activity and Stability under Visible Light Irradiation. *Applied Surface Science*. 409: 250-260. https://doi.org/10.1016/j.apsusc.2017.03.025.

[20] Zhou, L., W. Zhang, L. Chen, and H. Deng. 2017. Z-scheme Mechanism of Photogenerated Carriers for Hybrid Photocatalyst $Ag_3PO_4/g\text{-}C_3N_4$ in Degradation of Sulfamethoxazole. *Journal of Colloid and Interface Science*. 487: 410-417. https://doi.org/10.1016/j.jcis.2016.10.068.

[21] Liu, L., Y. Qi, J. Lu, S. Lin, W. An, Y. Liang, and W. Cui. 2016. A Stable Ag_3PO_4@g-C_3N_4 Hybrid core@shell Composite with Enhanced Visible Light Photocatalytic Degradation. *Applied Catalysis B: Environmental*. 183: 133-141. https://doi.org/10.1016/j.apcatb.2015.10.035.

[22] Zhang, C., L. Wang, F.Yuan, R. Meng, J. Chen, W. Hou, and H. Zhu. 2020. Construction of p-n Type $Ag_3PO_4/CdWO_4$ Heterojunction Photocatalyst for Visible-light-induced Dye Degradation. *Applied Surface Science*. 534: 147544. https://doi.org/10.1016/j.apsusc.2020.147544.

[23] Yu, Y., B. Yao, Y. Hea, B. Cao, Y. Ren, and Q. Sun. 2020. Piezo-enhanced Photodegradation of Organic Pollutants on Ag_3PO_4/ZnO Nanowires using Visible Light and Ultrasonic. *Applied Surface Science*. 528: 146819. https://doi.org/10.1016/j.apsusc.2020.146819.

[24] Yin, H., Y. Cao, T. Fan, M. Zhang, J. Yao, P. Li, S. Chen, and X. Liu. 2021. In Situ Synthesis of Ag_3PO_4/C_3N_5 Z-scheme Heterojunctions with Enhanced Visible-light-responsive Photocatalytic Performance for Antibiotics Removal. *Science of the Total Environment*. 754: 141926. https://doi.org/10.1016/j.scitotenv.2020.141926.

[25] Guo, X., C. Chen, S. Yin, L. Huang, and W. Qin. 2015. Controlled Synthesis and Photocatalytic Properties of Ag_3PO_4 Microcrystals. *Journal of Alloys and Compounds*. 619: 293-297. https://doi.org/10.1016/j.jallcom.2014.09.065.

[26] Deng, M. and Y. Huang. 2020. The Phenomena and Mechanism for the Enhanced Adsorption and Photocatalytic Decomposition of Organic Dyes with Ag_3PO_4/graphene Oxide Aerogel Composites. *Ceramics International*. 46(2): 2565-2570. https://doi.org/10.1016/j.ceramint.2019.09.128.

[27] Li, Y., L. Yu, N. Li, W. Yan, and X. Li. 2015. Heterostructures of Ag_3PO_4/TiO_2 Mesoporous Spheres with Highly Efficient Visible Light Photocatalytic Activity. *Journal of Colloid and Interface Science*. 450: 246-253. https://doi.org/10.1016/j.jcis.2015.03.016.

[28] Wibawa, P. J., M. Nur, M. Asy'ari, W. Wijanarka, H. Susanto, H. Sutanto, and H. Nur. 2021. Green Synthesized Silver Nanoparticles Immobilized on Activated Carbon Nanoparticles: Antibacterial Activity Enhancement Study and Its Application on Textiles Fabrics. *Molecules*. 26: 3790. https://doi.org/10.3390/molecules26133790.

[29] Fahimirad, S., F. Ajalloueian, and M. Ghorbanpour. 2019. Synthesis and Therapeutic Potential of Silver Nanomaterials Derived from Plant Extracts. *Ecotoxicology and Environmental Safety*, 168: 260-278. https://doi.org/10.1016/j.ecoenv.2018.10.017.

[30] Suryono, S., H. Hadiyanto, M. Yasin, R. Widyowati, M. Muniroh, A. Amalia. 2019. Effect of Frequency, Temperature, and Time of Sonication on Xanton Content of Mangosteen (Garcinia mangostana L.) Peel Extract through Ultrasound Assisted Extraction. *E3S Web of Conferences*. 125: 25006. https://doi.org/10.1051/e3sconf/201912525006.

[31] A. S. Zarena, K. Udaya Sankar. 2011. Xanthones Enriched Extracts from Mangosteen Pericarp Obtained by Supercritical Carbon Dioxide Process. *Separation and Purification Technology*. 80: 172-178. https://doi.org/10.1016/j.seppur.2011.04.027.

[32] Dewi, K. I. G. A. S. P., I. B. P. Manuaba, I. W. P. S. Yasa, and B. K. Satriyasa. 2018. Methanol Extract of Mangosteen Peel (Garcinia mangostana L.) Increase Activity Acetylcholinesterase and Glutathione Peroxidase and Reduce MDA in Diazinon Exposed Rat. *Bali Medical Journal*. 7(3): 741-743. https://doi.org/10.15562/bmj.v7i3.979.

[33] Karnaji and I. Nurhasanah. 2017. Photodegradation of Rhodamine B by using $ZnFe_2O_4$ Nanoparticles Synthesized through Precipitation Method. *IOP Conf. Series: Materials Science and Engineering*. 202: 012044. https://doi.org/10.1088/1757-899X/202/1/012044.

[34] Ariyanti, D., M. Maillot, and W. Gao. 2017. TiO_2 used as Photocatalyst for Rhodamine B Degradation under Solar Radiation. *International Journal of Modern Physics B*. 31(16-19): 1744095. https://doi.org/10.1142/S0217979217440957.

[35] Bi, Y., S. Ouyang, N. Umezawa, J. Cao, and J. Ye. 2011. Facet Effect of Single-crystalline Ag_3PO_4 Sub-microcrystals on Photocatalytic Properties. *Journal of the American Chemical Society*. 133: 6490-6492. https://doi.org/10.1021/ja2002132.

[36] Vidyasagar, C. C. and Y. A. Naik. 2016. Surfactant (PEG 400) Effects on Crystallinity of ZnO Nanoparticles. *Arabian Journal of Chemistry*. 9(4): 507-510. https://doi.org/10.1016/j.arabjc.2012.08.002.

[37] Xu, H., C. Wang, Y. Song, J. Zhu, Y. Xu, J. Yan, and Y. Song and H. Li. 2014. CNT/Ag_3PO_4 Composites with Highly Enhanced Visible Light Photocatalytic Activity and Stability. *Chemical Engineering Journal*. 241: 35-42. https://doi.org /10.1016/j.cej.2013.11.065.

[38] Ko, H. H., G. Yang, M. C. Wang, and X. Zhao. 2014. Isothermal Crystallization Kinetics and Effect of Crystallinity on the Optical Properties of Nanosized CeO_2 Powder. *Ceramics International*, 40(5): 6663-6671. https://doi.org/10.1016/j.ceramint.2013.11.126.

[39] Ghosh, M., P. Chowdhury, and A. K. Ray. 2020. Photocatalytic Activity of Aeroxide TiO_2 Sensitized by Natural Dye Extracted from Mangosteen Peel. *Catalysts*. 10(8): 917. https://doi.org/10.3390/catal10080917.

[40] Ma, J., Q. Liu, L. Zhu, J. Zou, K. Wang, M. Yang, and S. Komarneni. 2016. Visible Light Photocatalytic Activity Enhancement of Ag_3PO_4 Dispersed on Exfoliated Bentonite for Degradation of Rhodamine B. *Applied Catalysis B: Environmental*. 182: 26-32. https://doi.org/10.1016/j.apcatb.2015.09.004.

[41] Yang, S., D. Zhao, H. Zhang, S. Lu, L. Chen, and X. Yu. 2010. Impact of Environmental Conditions on the Sorption Behavior of Pb (II) in Na-bentonite Suspensions. *Journal of Hazardous Materials*. 183: 632-640. https://doi.org/10.1016/j.jhazmat.2010.07.072.

[42] Kurniawan, Y.S., M. R. G. Fahmi, and L. Yuliati. 2020. Isolation and Optical Properties of Natural Pigments from Purple Mangosteen Peels. *IOP Conf. Series: Materials Science and Engineering*. 833: 012018. https://doi.org/10.1088/1757-899X/833/1/012018.

[43] Astuti, Y., R. Andianingrum, Arnelli, A. Haris, and A. Darmawan. 2020. The Role of $H_2C_2O_4$ and Na_2CO_3 as Precipitating Agents on the Physichochemical Properties and Photocatalytic Activity of Bismuth Oxide. *Open Chemistry*. 18: 129-137. https://doi.org/10.1515 /chem-2020-0013.